

Universal magnetoresponse in QCD and $\mathcal{N}=4$ SYM

Gergely Endrődi,^{1,*} Matthias Kaminski,^{2,†}

Andreas Schäfer,^{3,‡} Jackson Wu,^{2,§} and Laurence Yaffe^{4,¶}

¹*Institute for Theoretical Physics, Goethe Universität Frankfurt,
D-60438 Frankfurt am Main, Germany*

²*Department of Physics and Astronomy,
University of Alabama, Tuscaloosa, AL 35487, USA*

³*Institut für Theoretische Physik, Universität Regensburg, 93040 Regensburg, Germany*

⁴*Department of Physics, University of Washington, Seattle, WA 98195-1560, USA*

Using recent lattice data on the thermodynamics of QCD in the presence of a background magnetic field, we show that the ratio of transverse to longitudinal pressure exhibits, to good accuracy, a simple scaling behavior over a wide range of temperature and magnetic field, essentially depending only on the ratio T/\sqrt{B} . We compare this QCD response to the corresponding magnetoresponse in maximally supersymmetric Yang Mills theory. Given suitable calibrations defining the comparison, we find excellent agreement. This may be viewed as a further test of the applicability of holographic models for hot QCD.

* endrodi@th.physik.uni-frankfurt.de

† mski@ua.edu

‡ andreas.schaefer@physik.uni-regensburg.de

§ jmwu@ua.edu

¶ yaffe@phys.washington.edu

CONTENTS

I. Introduction	3
II. Quantum field theory with an external magnetic field	5
A. Thermodynamics	5
B. Renormalization	8
III. Lattice quantum chromodynamics	10
IV. $\mathcal{N} = 4$ supersymmetric Yang Mills theory	13
V. Comparison of QCD and $\mathcal{N} = 4$ SYM	15
VI. Discussion	18
Acknowledgments	20
A. Magnetic field matching at high temperature	20
References	21

I. INTRODUCTION

Gauge-gravity duality has enabled quantitative studies of the dynamics of certain strongly coupled non-Abelian plasmas [1–4]. Despite the limitations of holographic models (involving large N_c , strong coupling limits, and supersymmetry), they have provided important insight into key properties of quark-gluon plasma as observed in relativistic heavy-ion collisions, including fast “thermalization” and the applicability of near-ideal hydrodynamics [5–9].

In this paper, we compare the magnetoresponse of QCD plasma and maximally supersymmetric Yang Mills ($\mathcal{N} = 4$ SYM) plasma — the non-Abelian plasma with the simplest holographic description. Specifically, we examine the change in thermodynamic properties induced by a homogeneous background magnetic field. The response to an applied magnetic field is a useful probe of the dynamics in many condensed matter systems. In our context, an examination of magnetoresponse is also motivated by work suggesting that electromagnetic fields (albeit transient) may have significant effects in heavy ion collisions [10, 11].

Holographic models have been found to describe rather accurately many aspects of strongly coupled QCD dynamics, despite the fact that QCD is neither conformal, supersymmetric, nor infinitely strongly coupled. Any reasonable measure of QCD coupling strength in experimentally accessible quark-gluon plasma is order unity, far from the infinite coupling limit, and $N_c = 3$ appears equally far from $N_c = \infty$. The apparent robustness of AdS/CFT predictions, despite these limitations, has prompted numerous investigations. It has been shown, for example, that finite coupling corrections in many thermal quantities are modest [12, 13], and that N_c dependence is essentially trivial, with extensive quantities simply scaling with the number of gauge fields [14, 15].

To investigate whether a similar robustness exists with respect to conformal symmetry it is natural to examine the effects of deformations which explicitly break conformal symmetry. Adding a background magnetic field is such a non-conformal deformation.

In the presence of an external electromagnetic field, the definition of the QCD contribution to the total stress-energy tensor depends on a choice of renormalization point. This issue is discussed in section II, which reviews basic properties of the stress-energy tensor of a quantum field theory when minimally coupled to a non-dynamical electromagnetic field.

For QCD magnetoresponse, we take as input results from recent high quality lattice gauge theory calculations of QCD thermodynamics for a wide range of background magnetic field B

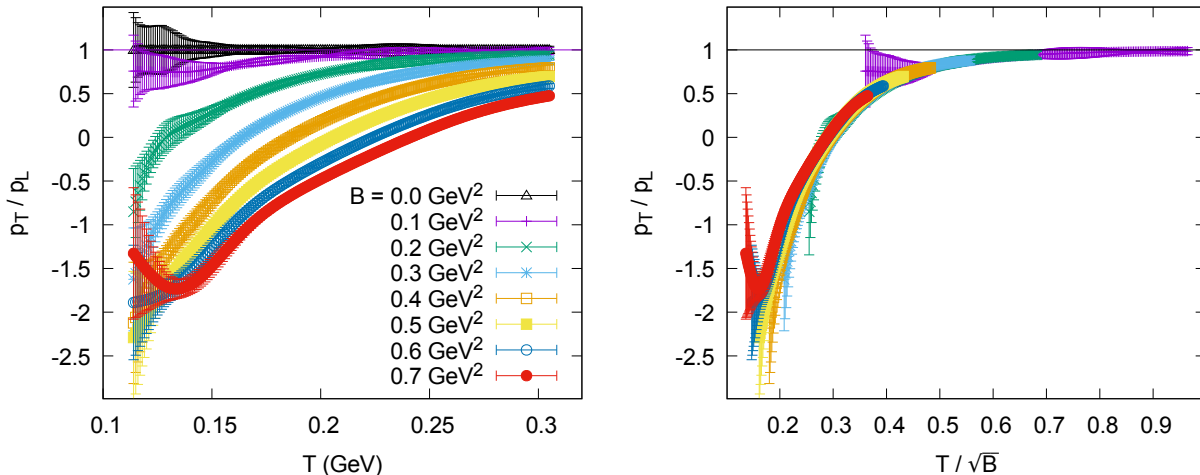


FIG. 1. The ratio $R \equiv p_T/p_L$ of transverse to longitudinal pressure in QCD, defined with renormalization point $\mu = \Lambda_H$, for various values of external magnetic field B . (See Section III for details.) Left panel: R plotted as a function of T . Right panel: R plotted as a function of T/\sqrt{B} . The different colors indicate different values of the magnetic field and are identical in the two panels.

and temperature T [16, 17]. A natural measure of anisotropy in the system is the transverse to longitudinal pressure ratio p_T/p_L , shown in the left panel of Fig. 1 as a function of T for different magnetic fields. Interestingly, we find that this ratio exhibits, to good accuracy, a simple scaling behavior over a wide range of temperature and magnetic field. As shown in the right panel of the same figure, when plotted as a function of T/\sqrt{B} data from widely differing values of T and B essentially collapse onto a single curve. The underlying lattice QCD data is discussed in more detail in Section III, (Deviations from this scaling behavior appear to be present at the lowest temperatures and highest magnetic fields, but the growth of the error bars precludes making any definitive statement about this region.)

In any conformal field theory,¹ the lack of intrinsic scales automatically implies that the magnetoresponse (appropriately defined) can only depend on the dimensionless ratio T/\sqrt{B} . So, having found near-universal scaling behavior in the QCD magnetoresponse, it is natural to compare this response to that of the simplest holographic model, namely conformal $\mathcal{N}=4$ SYM in the strong coupling and large N limit, for which the dual description reduces to 5D Einstein-Maxwell theory. We briefly review $\mathcal{N}=4$ SYM theory and its coupling to a background EM field in section IV, and then compare the QCD and $\mathcal{N}=4$ SYM

¹ See Ref. [18] for a careful discussion of the relation between scale invariance and full conformal symmetry.

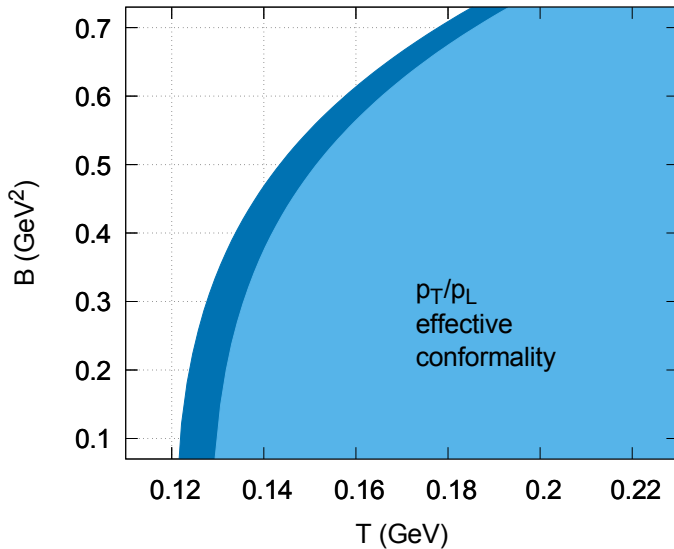


FIG. 2. Region of effective conformality, in the plane of temperature and magnetic field, of the QCD pressure anisotropy ratio p_T/p_L . Within the blue region QCD and $\mathcal{N}=4$ SYM, appropriately compared, give identical values for this ratio to within the error estimates of the lattice data. The dark blue band indicates the uncertainty in the border of this region arising from lattice errors.

magnetoresponse in Section V. A key issue, discussed in some detail, concerns how best to make such a comparison given the unavoidable renormalization point dependence of the quantities under study.

For impatient readers, our end result is shown graphically in Fig. 2. Within the shaded region of the temperature-magnetic field plane, the QCD and $\mathcal{N}=4$ SYM results for the pressure anisotropy ratio p_T/p_L , appropriately compared, are found to be identical to within the errors of the lattice data. Our final section VI discusses the implications of this result and possible future directions. An appendix contains a few details regarding a high temperature matching procedure for relating QCD and SYM quantities.

II. QUANTUM FIELD THEORY WITH AN EXTERNAL MAGNETIC FIELD

A. Thermodynamics

Consider a quantum field theory (QFT) minimally coupled to an external electromagnetic $U(1)$ gauge field A_μ^{ext} , with field strength $F_{\mu\nu}^{\text{ext}} = \partial_\mu A_\nu^{\text{ext}} - \partial_\nu A_\mu^{\text{ext}}$. A constant magnetic field $\mathbf{B} = B \mathbf{e}_z$ may be described by the standard choice $A_\mu^{\text{ext}} = \frac{1}{2}B(x^1\delta_\mu^2 - x^2\delta_\mu^1)$. The total action

of the theory may be written in the form

$$S = S_{\text{QFT}}(B) + S_{\text{EM}}(e, B), \quad S_{\text{EM}}(e, B) \equiv - \int d^4x \frac{B^2}{2e^2}, \quad (1)$$

where S_{EM} is the classical Maxwell action, specialized to a pure magnetic field, with e the (bare) electromagnetic coupling constant, and the QFT action $S_{\text{QFT}}(B)$ includes the minimal coupling to the background EM field.² Here and henceforth, we choose to scale the external gauge field A_μ^{ext} so that the electromagnetic coupling e does not appear in covariant derivatives, but instead e^2 is an inverse factor in the Maxwell action. Consequently, our B is the same as eB if a conventional perturbative scaling of the $U(1)$ field is used.³

From the action (1) (generalized to curved space) one derives the stress-energy tensor,

$$T^{\mu\nu} = -2 \frac{\delta S}{\delta g_{\mu\nu}} = T_{\text{QFT}}^{\mu\nu} + T_{\text{EM}}^{\mu\nu}, \quad (2)$$

where $T_{\text{QFT}}^{\mu\nu} = -2\delta S_{\text{QFT}}/\delta g_{\mu\nu}$ is the QFT contribution to the total stress-energy tensor, while

$$T_{\text{EM}}^{\mu\nu} = -2 \frac{\delta S_{\text{EM}}}{\delta g_{\mu\nu}} = \frac{1}{e^2} (F^{\mu\alpha} F^{\nu\beta} \eta_{\alpha\beta} - \frac{1}{4} \eta^{\mu\nu} F^{\alpha\beta} F_{\alpha\beta}), \quad (3)$$

is the standard Maxwell stress-energy tensor (in Minkowski space). Specialized to a constant magnetic field in the z -direction, $T_{\text{EM}}^{\mu\nu} = \frac{B^2}{2e^2} \text{diag}(+1, +1, +1, -1)$.

In a homogeneous equilibrium state, viewed in a rest frame (with vanishing momentum density) aligned with the magnetic field, diagonal elements of the expectation value of the stress-energy tensor can be interpreted as the proper energy density ϵ , and pressures (or diagonal stresses) p_x, p_y, p_z along the x -, y -, z -directions, respectively,

$$\langle T^{\mu\nu} \rangle = \begin{pmatrix} \epsilon & 0 & 0 & 0 \\ 0 & p_x & 0 & 0 \\ 0 & 0 & p_y & 0 \\ 0 & 0 & 0 & p_z \end{pmatrix}. \quad (4)$$

The magnetic field defines a preferred direction in space, and induces an anisotropy between the longitudinal pressure $p_L \equiv p_z$ and transverse pressure $p_T \equiv p_x = p_y$. (Rotational symmetry about the magnetic field direction implies that $p_x = p_y$.) The relation between the pressure(s) and energy density constitutes the equation of state of the system.

² In this section, we work in Minkowski space with metric $\eta_{\mu\nu} = \text{diag}(-1, +1, +1, +1)$.

³ In particular, our magnetic field B corresponds to eB in Ref. [16].

Similarly to the action (1), the thermodynamic grand potential (or Landau free energy),

$$\mathcal{F} \equiv -T \ln \mathcal{Z}, \quad (5)$$

may be separated into QFT and EM contributions,

$$\mathcal{F} = \mathcal{F}_{\text{QFT}}(B) + \mathcal{F}_{\text{EM}}(e, B), \quad \mathcal{F}_{\text{EM}}(e, B) = \mathcal{V} \frac{B^2}{2e^2}, \quad (6)$$

with $\mathcal{V} = L_x L_y L_z$ the spatial volume. This separation, by definition, places all the response to the applied magnetic field in the QFT contribution to the free energy. Let $f_{\text{QFT}} = \mathcal{F}_{\text{QFT}}/\mathcal{V}$ and $f_{\text{EM}} = \mathcal{F}_{\text{EM}}/\mathcal{V}$ denote the corresponding free energy densities. Derivatives of the free energy density f_{QFT} with respect to the temperature or magnetic field define the entropy density and magnetization, respectively,

$$s = -\frac{\partial f_{\text{QFT}}}{\partial T}, \quad M = -\frac{\partial f_{\text{QFT}}}{\partial B}. \quad (7)$$

Similarly, pressures are defined by the response of the system to compression in a given direction,

$$p_i = -\frac{L_i}{\mathcal{V}} \frac{\partial \mathcal{F}_{\text{QFT}}}{\partial L_i}. \quad (8)$$

In the thermodynamic limit, for homogeneous systems, the pressure is normally just minus the free energy density, since the free energy is extensive in the volume. But with a background magnetic field, one must specify what is to be held fixed in the partial derivative defining the pressure (8) [16]. The microscopic definition (4) of pressures as stress-energy eigenvalues corresponds to a thermodynamic definition in which the effect of compression is evaluated at a fixed magnetic flux $\Phi = B L_x L_y$.⁴ Consequently, the longitudinal and transverse pressures differ,

$$p_L = -f_{\text{QFT}}, \quad p_T = p_L - M \cdot B. \quad (9)$$

The thermodynamic relation $f_{\text{QFT}} = \epsilon - Ts$ implies that the entropy and energy densities s and ϵ are related via

$$s = \frac{\epsilon + p_L}{T}. \quad (10)$$

⁴ To see this, note that the metric variation defining the stress-energy (2) leaves unchanged the EM flux across any 2-surface, $\Phi = \int_{\Sigma} F$, since integration of a two-form is metric independent.

A final quantity of interest is the interaction measure I , which is (minus) the trace of the stress-energy tensor

$$I = -\langle T^\mu_\mu \rangle = \epsilon - 2p_T - p_L = \epsilon - 3p_L + 2M \cdot B. \quad (11)$$

In a CFT, such as $\mathcal{N}=4$ SYM, conformal symmetry implies that the stress-energy tensor is traceless. However, adding an external magnetic field B is a non-conformal deformation of the theory and induces a non-zero trace, and hence a nonzero interaction measure. For $\mathcal{N}=4$ SYM (coupled to the external field in the manner described below in section IV),

$$T^\mu_\mu = -\frac{N_c^2 - 1}{4\pi^2} B^2. \quad [\mathcal{N}=4 \text{ SYM}] \quad (12)$$

For an asymptotically free theory like QCD, the stress-energy trace has an intrinsic contribution from the running of the coupling (and quark masses terms), plus the additional contribution from the external magnetic field. Neglecting quark masses,

$$T^\mu_\mu = -\beta(g^{-2}) \frac{1}{4} \text{tr} G_{\mu\nu}^2 - \tilde{\beta}(e^{-2}) \frac{1}{2} B^2, \quad [\text{QCD}] \quad (13)$$

where $G_{\mu\nu}$ is the gluon field strength, $\beta(g^{-2}) \equiv \mu \partial_\mu g^{-2} = 9/(4\pi^2) + \mathcal{O}(g^2)$ is the renormalization group β -function for the $SU(3)$ inverse gauge coupling (with three quark flavors), and $\tilde{\beta}(e^{-2}) \equiv \mu \partial_\mu e^{-2} = -1/(3\pi^2) + \mathcal{O}(g^2)$ is the corresponding electromagnetic β -function arising from the three light quark flavors of QCD.

B. Renormalization

In interacting quantum field theories, bare parameters of the action undergo multiplicative renormalization which introduces dependence on an arbitrary renormalization point μ .⁵ In particular, the renormalized electromagnetic coupling e^2 acquires logarithmic scale dependence and satisfies a QED-like renormalization group equation,

$$\mu \frac{d}{d\mu} e^{-2} \equiv \tilde{\beta}(e^{-2}) = -2b_1 \times [1 + \mathcal{O}(g^2)], \quad (14)$$

with positive coefficient b_1 . Explicitly, for QCD,

$$b_1 = \frac{N_c}{12\pi^2} \sum_f q_f^2 = \frac{1}{6\pi^2}, \quad [\text{QCD}] \quad (15a)$$

⁵ With our definition of the magnetic field B , the Ward-Takahashi identity shows that B receives no wavefunction renormalization and is scale independent.

where q_f denotes the electromagnetic charge assignments (i.e., EM charges in units of e) of each quark flavor, and the explicit final form is specialized to three flavor QCD. For $\mathcal{N}=4$ SYM theory,

$$b_1 = \frac{N_c^2 - 1}{24\pi^2} \left[\sum_w q_w^2 + \frac{1}{2} \sum_s q_s^2 \right], \quad [\mathcal{N}=4 \text{ SYM}] \quad (15b)$$

where the sums run over all charged Weyl fermions w and charged scalars s with q_w and q_s denoting the corresponding electromagnetic charge assignments. If the electromagnetic field is regarded as classical (so that EM quantum fluctuations are neglected) then the higher order corrections in the β -function (14) are independent of e^2 . For QCD in a background magnetic field, the EM β -function has higher order corrections proportional to the non-Abelian coupling g^2 , while for $\mathcal{N}=4$ SYM (in a background field), no higher order corrections appear in the EM β -function (14) due to a supersymmetric non-renormalization theorem. Neglecting any such higher order corrections, the solution to the renormalization group equation (14) shows the usual logarithmic scale dependence,

$$e(\mu_1)^{-2} = e(\mu_2)^{-2} - 2b_1 \ln(\mu_1/\mu_2). \quad (16)$$

Physical observables, like the total free energy, are necessarily independent of the renormalization point μ . However, the separation (6) of the free energy into QFT and background EM contributions requires choosing the scale at which to evaluate the coupling e appearing in the background EM contribution. So this separation is more properly written as

$$f = f_{\text{QFT}}(B, \mu) + f_{\text{EM}}(e(\mu), B), \quad (17)$$

with the scale dependence of $f_{\text{QFT}}(B, \mu)$ necessarily canceling that of the EM term, so that

$$\mu \frac{d}{d\mu} f_{\text{QFT}}(B, \mu) = b_1 B^2. \quad (18)$$

Similarly, the QFT stress-energy tensor acquires scale dependence,

$$\mu \frac{d}{d\mu} T_{\text{QFT}}^{\alpha\beta} = 2b_1 \left(F^{\alpha\gamma} F^{\beta\delta} \eta_{\gamma\delta} - \frac{1}{4} \eta^{\alpha\beta} F^{\gamma\delta} F_{\gamma\delta} \right), \quad (19)$$

which precisely cancels the scale dependence of the EM stress-energy tensor. Hence,

$$\epsilon(\mu') - \epsilon(\mu) = b_1 B^2 \ln \frac{\mu'}{\mu}, \quad (20a)$$

$$p_T(\mu') - p_T(\mu) = b_1 B^2 \ln \frac{\mu'}{\mu}, \quad (20b)$$

$$p_L(\mu') - p_L(\mu) = -b_1 B^2 \ln \frac{\mu'}{\mu}. \quad (20c)$$

This scale dependence induced by the separation of QFT response from the background EM contributions is unavoidable, since the background field contributions (for realistic values of the electromagnetic coupling) are orders of magnitude larger than the matter-induced response [17] and would otherwise overshadow interesting features in the magnetic field dependence of the QFT response.

III. LATTICE QUANTUM CHROMODYNAMICS

We consider QCD with $2 + 1$ flavors of dynamical quarks with physical masses. The quarks have their usual electric charge assignments, $q_u = +2/3$ and $q_d = q_s = -1/3$. The action has the form (1), with $S_{\text{QFT}} = S_{\text{QCD}}$ and covariant derivatives augmented to include the background $U(1)_{\text{EM}}$ gauge field. The lattice regularized Euclidean functional integral was simulated non-perturbatively using a staggered fermion discretization and three different lattice spacings. Details of the lattice discretization and associated methods are described in Ref. [17].

The lattice QCD results were obtained using a renormalization point $\mu = \Lambda_H$, where $\Lambda_H = 120(9)$ MeV is a non-perturbatively determined hadronic scale defined by the condition that at $T = 0$ there be no $\mathcal{O}(B^2)$ contribution to the matter free energy. In other words, the total free energy (the sum of matter and magnetic contributions) equals $\frac{1}{2}B^2/e^2(\Lambda_H) + \mathcal{O}(B^4)$ in the zero temperature limit. For nonzero temperatures, the $\mathcal{O}(B^2)$ contribution to the matter free energy becomes nonzero, i.e., the system develops a non-trivial magnetic permeability.

We begin the discussion with the anisotropic pressure components p_T and p_L . To facilitate a comparison with SYM theory, it is natural to consider the dimensionless ratio

$$R \equiv p_T/p_L. \quad (21)$$

This combination was shown as a function of the temperature for various values of magnetic field B in the left panel of Fig. 1. Notice that the longitudinal pressure p_L is always positive, so the ratio R remains finite for all T and B . For low magnetic fields the ratio $R \approx 1$, signaling the near-isotropy of the system. As the field B grows the anisotropy becomes more pronounced and the ratio R shifts away from unity — in fact it becomes negative when the transverse pressure p_T changes sign (and becomes a “suction”) for strong magnetic fields [17].

A remarkable feature of the results for $R(B, T, \Lambda_H)$ is their near-universal nature when expressed in terms of the dimensionless variable T/\sqrt{B} . This is shown in the right panel Fig. 1, which plots the same data with the exception of the $B = 0$ set. The data from different values of the magnetic field all collapse onto a single curve. (As noted earlier, small deviations from this scaling behavior may be present at the lowest temperatures and highest magnetic fields, but the growth of error bars in this regime prevents any definitive statement.) This indicates an apparent universality analogous to what one would expect, a-priori, only in conformal theories. In QCD the ratio R is in general a function of two independent dimensionless parameters,⁶

$$R(B, T, \Lambda_H) = r(T/\sqrt{B}, \Lambda_H/\sqrt{B}). \quad (22)$$

The apparent near absence of any significant dependence on Λ_H/\sqrt{B} motivates us to compare the magnetoresponse of QCD to that of conformal SYM theory, for which T/\sqrt{B} is the only relevant dimensionless ratio.

An important question is how the near-universality of p_T/p_L is affected by a change in the renormalization point. We consider a general choice,

$$\mu(c_T, c_\Lambda, c_B) \equiv \sqrt{c_T T^2 + c_B |B| + c_\Lambda \Lambda_H^2}, \quad (23)$$

involving the three underlying scales $\{T, B, \Lambda_H\}$ characterizing the equilibrium state, parameterized by three coefficients c_T , c_B and c_Λ . For a quantitative description we introduce a measure D of the deviation from universality,

$$D \equiv \frac{1}{N} \sum_{b, b'} \sum_t \frac{[r(t, b) - r(t, b')]^2}{\sigma^2(t, b) + \sigma^2(t, b')}, \quad t \equiv \frac{T}{\sqrt{B}}, \quad b \equiv \frac{\Lambda_H}{\sqrt{B}}, \quad (24)$$

where σ denotes the error of the ratio r and the sum extends over all points available from the lattice study of Ref. [17]. The integer N counts the number of terms in the resulting sums. With this normalization, $D \lesssim 1$ indicates that the curves for different magnetic fields all overlap each other within errors. Additionally, the inherent uncertainty on D is of order unity. The deviation D is plotted in Fig. 3 as a heat map in the space of the coefficients c_B , c_T and c_Λ . The left panel of the figure shows the $c_B = 0$ slice, while the right panel shows the orthogonal $c_\Lambda = 0$ slice.⁷

⁶ We neglect to indicate explicitly additional dependence on the ratios of quark masses to Λ_H .

⁷ The heat map of D remains very similar if one instead uses a parameterization of the renormalization point which is analytic in the magnetic field, $\mu = (c_T T^4 + c_B B^2 + c_\Lambda \Lambda_H^4)^{1/4}$.

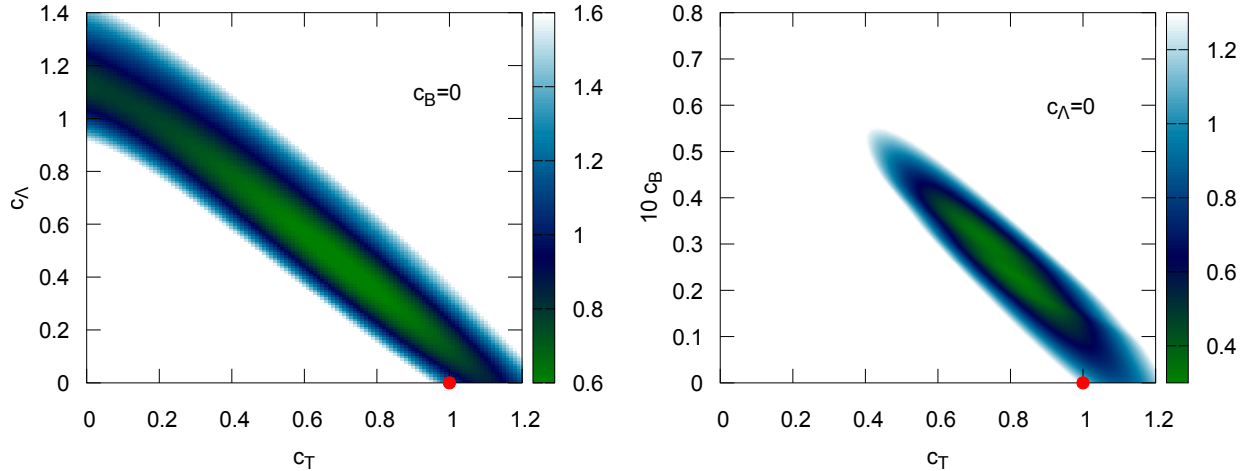


FIG. 3. Heat map of the deviation from universality, D , as a function of c_T and c_B for fixed $c_B = 0$ (left panel), and as a function of c_T and c_A for fixed $c_A = 0$ (right panel). The red dot indicates the choice of $\mu = T$. The uncertainty in the value of D is of order unity. Inside the dark colored regions, where $D \lesssim 1$, universality holds to within the error bars of the lattice data.

The ansatz (23), reflecting the presence of three different potentially relevant underlying scales, is a natural form for parameterizing a dominantly relevant scale in QCD. The appearance of Λ_H reflects the intrinsic lack of scale symmetry in QCD (even in the limit of massless quarks). In a conformal theory, there is no intrinsic energy scale, and hence no equivalent of the QCD scale Λ_H . A natural question to ask is whether the apparent universality in our lattice data remains evident when c_A is small or zero. As indicated in the left panel of Fig. 3, this is indeed the case. The region of minimal deviation from universality is found to be centered around the point $(c_T, c_A) = (0.70, 0.46)$, but it extends out to include, for example, the purely temperature-driven renormalization point $\mu = T$.

Therefore, in the following we set c_A to zero, so that a comparison to $\mathcal{N}=4$ SYM theory will be straightforward. As shown in the right panel of Fig. 3, for vanishing c_A the minimum of D defines a valley along the line $c_B = 0.087 - 0.084 c_T$. Below we will compare QCD to the SYM theory along this valley.

As illustrated in Fig. 4, other dimensionless ratios, such as p_L/ϵ or p_T/ϵ , have substantial dependence on Λ_H/\sqrt{B} and do not exhibit the near universality seen in the pressure anisotropy ratio p_T/p_L . Given the connection (11) between the trace anomaly and the interaction measure $I = \epsilon - 2p_T - p_L$, this surely reflects the substantial growth of the interaction

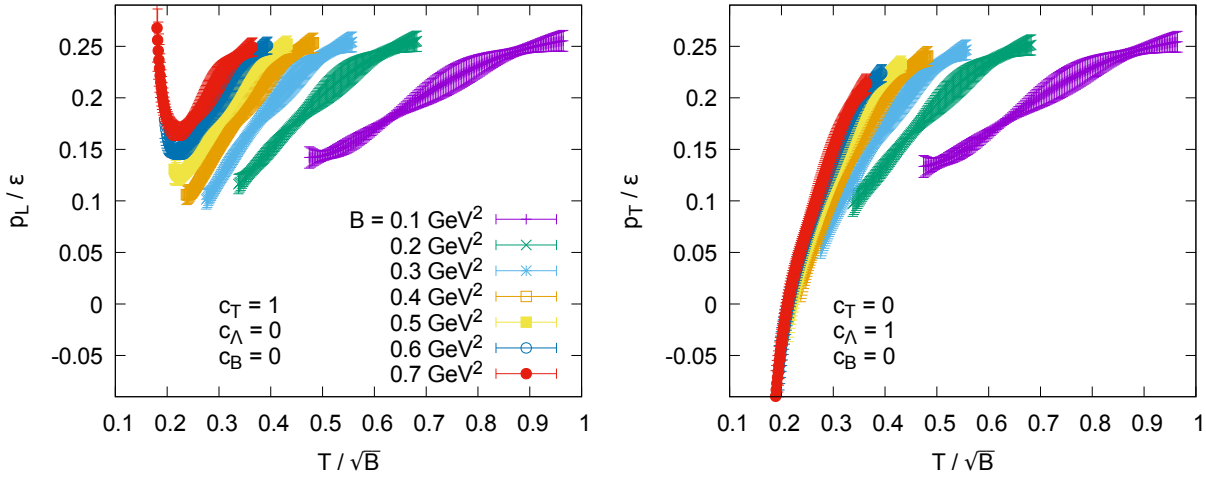


FIG. 4. Ratios p_L/ϵ (left panel) and p_T/ϵ (right panel) evaluated at renormalization point $\mu = \Lambda_H$ for various values of the magnetic field B , and plotted as a function of T/\sqrt{B} . Unlike the ratio p_T/p_L , no near universal behavior is observed in either ratio involving the energy density.

measure in QCD as the temperature approaches the confinement transition due to the intrinsic violation of scale invariance in QCD [19, 20], a feature not present in conformal $\mathcal{N} = 4$ SYM.

IV. $\mathcal{N} = 4$ SUPERSYMMETRIC YANG MILLS THEORY

We consider maximally supersymmetric ($\mathcal{N} = 4$) $SU(N_c)$ Yang-Mills theory, in the limit of large N_c and large 't Hooft coupling, $\lambda \gg 1$, coupled to a background “electromagnetic” $U(1)$ gauge field. To define this coupling, we choose the same $U(1)$ subgroup of the $SU(4)$ global R -symmetry which was used in Ref. [21]. Specifically,

$$q_w^\alpha = (3, -1, -1, -1)/\sqrt{3}, \quad q_s^a = (2, 2, 2)/\sqrt{3}, \quad (25)$$

are the respective charge assignments for the four Weyl fermions and three complex scalars of $\mathcal{N} = 4$ SYM. With these assignments, the $U(1)$ β -function coefficient (15b) becomes

$$b_1 = \frac{N_c^2 - 1}{4\pi^2}. \quad [\mathcal{N} = 4 \text{ SYM}] \quad (26)$$

(However, as discussed in the next section, when comparing with QCD we will rescale the above charge assignments by an adjustable factor.)

Equilibrium states of this theory, in the presence of a homogeneous background magnetic field, have a dual gravitational description given by magnetic black brane solutions first computed by D'Hoker and Kraus [22]. These are solutions of 5D Einstein-Maxwell theory, which is a consistent truncation of type IIB supergravity. The Einstein-Maxwell action

$$S = \frac{1}{16\pi G_5} \int d^5x \sqrt{-g} [\mathcal{R} - 2\Lambda - L^2 \mathcal{F}_{MN} \mathcal{F}^{MN}] + \theta \int d^5x \mathcal{A} \wedge \mathcal{F} \wedge \mathcal{F}, \quad (27)$$

where $M, N = 0, \dots, 4$ are the 5D spacetime indices, g is the metric, \mathcal{R} is the Ricci scalar, $G_5 = \frac{\pi}{2} L^3 / (N_c^2 - 1)$ is the 5D Newton gravitational constant, $\Lambda = -6L^{-2}$ is the cosmological constant and $\mathcal{F} = d\mathcal{A}$ is the five-dimensional electromagnetic field strength. The reduction from IIB supergravity leads to a specific value for the Chern-Simons coupling θ , but this term vanishes identically for our solutions of interest and may be ignored. Solutions to the gravitational theory (27) representing uncharged (magnetic) black branes may be described by a metric of the form [22],

$$ds^2 = -U(r) dt^2 + \frac{dr^2}{U(r)} + e^{2V(r)} (dx^2 + dy^2) + e^{2W(r)} dz^2, \quad (28)$$

plus a bulk field strength

$$\mathcal{F} = B dx \wedge dy, \quad (29)$$

representing a constant magnetic field of strength B . The metric functions U , V and W depend only on the radial coordinate r , and must be computed numerically. These functions have the near-boundary ($r \rightarrow \infty$) asymptotic behavior,

$$U(r) = r^2/L^2 + 2(a_4 - \frac{1}{3}B^2 \ln r/L) L^6/r^2 + \mathcal{O}(r^{-6} \ln^2 r/L), \quad (30a)$$

$$V(r) = \ln(r/L) + \frac{1}{2}(b_4 + \frac{1}{3}B^2 \ln r/L) L^8/r^4 + \mathcal{O}(r^{-8} \ln^2 r/L), \quad (30b)$$

$$W(r) = \ln(r/L) - (b_4 + \frac{1}{3}B^2 \ln r/L) L^8/r^4 + \mathcal{O}(r^{-8} \ln^2 r/L). \quad (30c)$$

The subleading terms in these near-boundary expansions determine the (expectation value of the) $\mathcal{N}=4$ SYM stress-energy tensor [21]. Specifically,

$$\langle T^{tt} \rangle = \epsilon = \kappa \left(-\frac{3}{2}a_4 + \frac{1}{2}B^2 \ln \mu L \right), \quad (31a)$$

$$\langle T^{xx} \rangle = \langle T^{yy} \rangle = p_T = \kappa \left(-\frac{1}{2}a_4 + b_4 - \frac{1}{4}B^2 + \frac{1}{2}B^2 \ln \mu L \right), \quad (31b)$$

$$\langle T^{zz} \rangle = p_L = \kappa \left(-\frac{1}{2}a_4 - 2b_4 - \frac{1}{2}B^2 \ln \mu L \right), \quad (31c)$$

with all off-diagonal components vanishing. Here $\kappa \equiv (N_c^2 - 1)/(2\pi^2)$ and μ , once again, is the arbitrary renormalization point used to separate the SYM and background EM contributions to the total stress-energy tensor. For further details, see Refs. [21, 23].

V. COMPARISON OF QCD AND $\mathcal{N}=4$ SYM

To compare lattice QCD results with thermodynamic data for $\mathcal{N}=4$ SYM calculated via holography, one must decide how best to adjust for the differing field content of the two theories. Specifically, in making this comparison should the SYM charge assignments be rescaled? The overall normalization of our SYM charge assignments (25) was merely a convenient choice which corresponds to the absence of additional numerical factors multiplying the Maxwell term in the dual gravitational action (27) [21]. A uniform rescaling of charge assignments is equivalent to a rescaling of the magnetic field, so this question is the same as asking whether comparisons are most usefully made at coinciding values of magnetic field, as it was introduced in the gravitational action (27), or whether it is appropriate to first rescale the background magnetic field added to SYM theory.

As long as the background electromagnetic field is treated as classical, the normalization of SYM charge assignments is arbitrary, as there is no intrinsic scale available to define physical units in which to measure a magnetic field. In other words, there is no quantization of EM charges or magnetic fluxes. Hence, it is completely appropriate to rescale SYM charge assignments, or equivalently rescale the magnetic field, $B \rightarrow B/\xi$ for some choice of ξ , when comparing with QCD. (In contrast, temperature may be regarded as having a common operational meaning in both theories, so no rescaling of temperature is performed.) The key question is how should one choose this charge (or magnetic field) scale factor ξ ?

From our earlier discussion (sec. II B) of renormalization point dependence, one seemingly natural possibility to consider is scaling the SYM charge assignments so that the leading coefficient b_1 in the $U(1)$ β -function (15) coincides between QCD and SYM. This would require scaling the SYM charge assignments inversely with N_c so as to compensate for the difference in the number of charged degrees of freedom. However, this choice is neither necessary nor helpful, as one can always first define rescaled stress-energy tensors, $\tilde{T}^{\mu\nu} \equiv T^{\mu\nu}/b_1$, in both QCD and SYM, so that the rescaled tensors satisfy identical renormalization group equations. Since we are comparing dimensionless ratios such as p_T/p_L , such an overall rescaling of $T^{\mu\nu}$ has no effect on the comparison between theories.

Another possible approach involves matching the magnetoresponse in the asymptotically high temperature limit. As discussed in appendix A, if one considers the entropy density (which is independent of the renormalization point μ) and demands that the relative con-

tribution of the $\mathcal{O}(B^2)$ terms coincide, so that

$$\left. \frac{s(B, T)}{s(0, T)} \right|_{\text{QCD}} = \left. \frac{s(B/\xi, T)}{s(0, T)} \right|_{\text{SYM}} + \mathcal{O}(B^4), \quad (32)$$

then this condition leads to a scale factor choice $\xi = \sqrt{19/3} \approx 2.5$.

This value for the charge rescaling defines an arguably sensible scheme for comparing our two theories. However, it uses information from asymptotically high temperature QCD which is far from the regime of a few times T_c where it is appropriate to view real quark-gluon plasma as a strongly coupled near-conformal fluid. Consequently, our preferred approach is the simplest: we just treat the charge rescaling factor ξ as a free parameter, and find the value which minimizes the difference between the QCD and SYM results for the pressure ratio $R = p_T/p_L$. More precisely, we first evaluate this pressure ratio (as a function of B and T), in both theories at a common renormalization point $\mu = (c_T T^2 + c_B |B|)^{1/2}$ which lies along the valley defined by $c_B = 0.087 - 0.084 c_T$. As shown in Fig. 3, along this valley the QCD ratio R is essentially a function of only the single variable T/\sqrt{B} . We then define a deviation ΔR between the QCD pressure ratio and that of SYM,

$$\Delta R(\xi, c_T) \equiv \frac{1}{N} \sum_{B, T} \frac{\left[R^{\text{QCD}}(T/\sqrt{B}; \mu(c_T)) - R^{\text{SYM}}(T \sqrt{\xi/B}; \mu(c_T)) \right]^2}{\sigma^2(T, B)}, \quad (33)$$

with the SYM magnetic field rescaled by a adjustable factor ξ and c_B determined by c_T along the aforementioned valley. Only lattice QCD data points with $T > 150$ MeV are included in this sum, as lower temperatures probe the hadronic phase of QCD, not the deconfined plasma phase. As in our earlier measure D of the deviation from universality (24), σ denotes the lattice error of the ratio R , and N is the number of terms in the sum. A value less than unity for the deviation, $\Delta R < 1$, indicates agreement between the two theories to within the errors of the lattice results, and the inherent uncertainty in ΔR is of order unity.

Our results for ΔR are plotted in Fig. 5. As clearly seen in the figure, ΔR develops a minimum around $\xi = 4.3$ and $c_T = 0.69$ (implying $c_B = 0.029$), with its minimum value well below 1. The red dot on the right of Fig. 5 indicates a choice of the high temperature motivated rescaling factor $\xi = 2.5$ discussed above combined with $c_T = 1$. At this point ΔR is large compared to 1, indicating much less satisfactory matching between theories with this choice of rescaling.

A direct comparison of the pressure anisotropy ratio p_T/p_L in QCD and $\mathcal{N}=4$ SYM is displayed in Fig. 6 using choices of renormalization point and charge rescaling which

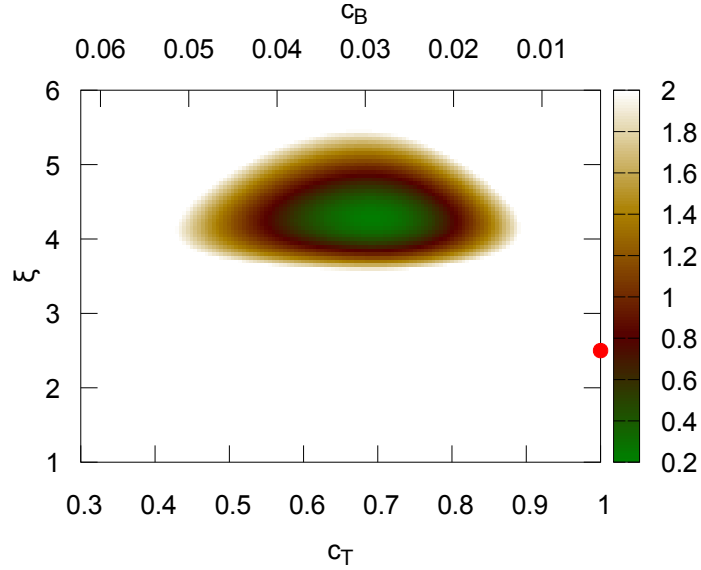


FIG. 5. The normalized deviation ΔR of the QCD and $\mathcal{N}=4$ SYM results for p_T/p_L , plotted as a function of the SYM charge rescaling factor ξ and the value of c_T defining the renormalization point (with c_B correspondingly fixed to lie along the QCD valley of near-universality). The red dot indicates the high temperature motivated choice $\mu = T$ and $\xi = 2.5$.

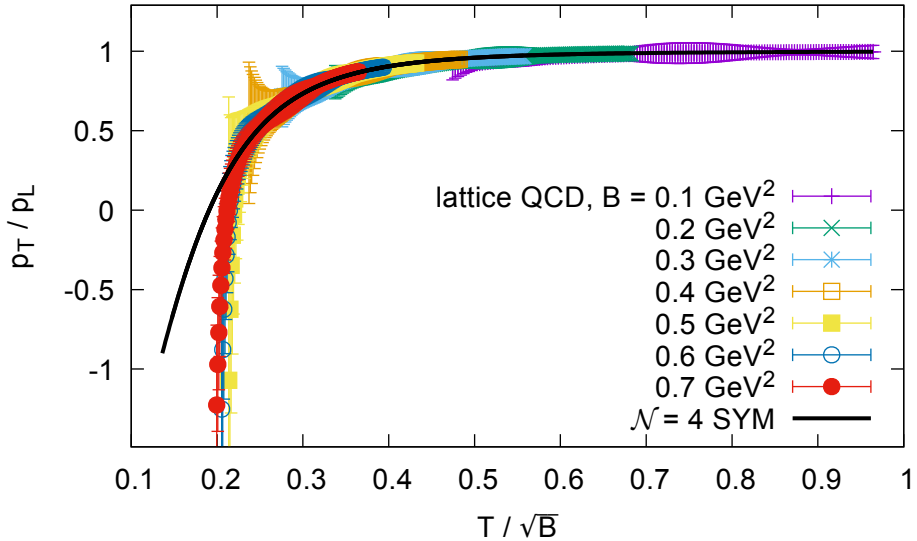


FIG. 6. The ratio p_T/p_L from lattice QCD as a function of T/\sqrt{B} at optimal universality – i.e. for a renormalization scale parameterized by $c_B = 0.029$, $c_T = 0.69$ and $c_\Lambda = 0$. Also included is the holographic pressure ratio computed at the same renormalization scale and with the electric charge normalization factor $\xi = 4.3$.

minimize ΔR , namely $(c_T, c_B) = (0.69, 0.029)$ (with $c_\Lambda = 0$), and $\xi = 4.3$. In addition to the universal scaling of the lattice QCD data, one sees that the SYM curve lies atop the error bars of the QCD data for all $T/\sqrt{B} \gtrsim 0.22$, or equivalently for magnetic fields up to $\approx 21 T^2$. Deviations of the QCD data from the SYM curve are present, and are significant, for $T/\sqrt{B} \lesssim 0.22$. This reflects the limit of the region where it makes sense to model QCD plasma as a conformal fluid. Figure 2, shown in the Introduction, gives a global view of the region of the temperature-magnetic field plane, in physical units, in which agreement between the QCD and SYM magnetoresponse holds to within the error estimate on the lattice QCD value of p_T/p_L . Agreement was inevitable at large T/\sqrt{B} where the pressure ratio in both theories necessarily approaches unity. But excellent agreement down to rather small temperatures, or up to quite large magnetic fields where the deviation of the pressure anisotropy from unity is substantial, is surprising. More precisely, it is remarkable that a choice of renormalization scale exists for which the pressure ratio in QCD and SYM, suitably compared, displays a common conformal behavior over such a substantial range of temperature and magnetic field.

VI. DISCUSSION

In this work, we analyzed data from a recent lattice gauge theory calculation of the thermodynamics of a QCD plasma placed in an external magnetic field. Except at asymptotically high temperatures, $T \gg \Lambda_{\text{QCD}}$, observables in QCD will generically have independent non-trivial dependence on the value of both temperature and magnetic field (relative to Λ_{QCD}). Moreover, separating the QCD contribution from the classical Maxwell contribution to the stress-energy tensor necessarily introduces dependence on an arbitrary renormalization point μ , as discussed in section II B. So in the presence of a non-zero magnetic field, at any physically accessible temperature, the transverse to longitudinal pressure ratio $R = p_T/p_L$ should be expected to display non-trivial dependence on multiple dimensionless ratios, for example T/\sqrt{B} , T/Λ_{QCD} , and T/μ . Choosing the renormalization point to depend in some dimensionally consistent fashion on the physical scales T , \sqrt{B} , and Λ_{QCD} still leaves two independent dimensionless ratios on which the pressure ratio should depend. However, as shown in Fig. 1, we find that for suitable choices of renormalization point the pressure anisotropy p_T/p_L exhibits scale invariance to within the error estimates of the

lattice data, with functional dependence only on the ratio T/\sqrt{B} . A more careful study of the deviations from universality identified an optimal choice of renormalization point, $\mu = (0.69T^2 + 0.029|B|)^{1/2}$ (given our specific measure (24) on the deviation).

Scale invariance is, of course, a feature of conformal field theories. Our observed near-perfect scale invariance in the QCD pressure anisotropy motivated a comparison with the pressure anisotropy in the simplest four dimensional conformal gauge theory, $\mathcal{N}=4$ supersymmetric Yang-Mills (SYM) theory, when this theory is placed in an external magnetic field. Specifically, we compared with $\mathcal{N}=4$ SYM in the large N_c and strong coupling limit, for which a dual gravitational description is available. After a simple matching of the electromagnetic couplings of the two theories, the SYM pressure anisotropy was found to agree with that of QCD over a wide range of temperature and magnetic field values, as shown in Fig. 6. This agreement persists at unexpectedly low temperatures and large magnetic fields. (Growing error bars on the lattice data make the comparison inconclusive below $T/\sqrt{B} < 0.2$.) The region where the pressure ratios of the two theories coincide was visualized in Fig. 2. It must be noted, however, that ratios of other thermodynamic quantities do not exhibit the same universal scaling behavior seen in the pressure anisotropy p_T/p_L . For ratios involving the energy density such as p_T/ϵ or p_L/ϵ , no choice of renormalization scale creates an overlap of data from different values of external field anywhere near as striking as that seen in the pressure anisotropy ratio. This, presumably, reflects the substantial peak in the thermal expectation value of the QCD trace anomaly, $I = \epsilon - 2p_T - p_L$, near the QCD confinement transition, which is not reproduced by $\mathcal{N}=4$ SYM.

Although our analysis has exclusively involved equilibrium quantities (for which lattice QCD calculations are possible), the region of “effective conformality” shown in Fig. 2 is presumably also the region in which the long wavelength dynamics of QCD plasma is reasonably well described by conformal hydrodynamics. Outside this region, effects of scale non-invariance should be increasingly important, implying significant bulk viscosity effects in QCD hydrodynamic response.

This work adds the pressure anisotropy magnetoresponse, described by a non-trivial scaling function of T/\sqrt{B} , to the set of thermal observables in QCD which are well-reproduced by strongly coupled $\mathcal{N}=4$ SYM, the simplest (four dimensional) conformal gauge theory with a holographic description. It also reveals the limitations of modeling hot QCD plasma as a conformal fluid when thermodynamic ratios involving the energy density are examined.

This limitation is unsurprising, given what is known about the temperature dependence of the trace anomaly expectation value.

It would be interesting to explore extensions of this work involving comparisons with other strongly coupled theories having holographic descriptions which are closer to QCD than $\mathcal{N}=4$ SYM. Possibilities include $\mathcal{N}=2^*$ SYM [24–27] and other mass deformations of $\mathcal{N}=4$ SYM, cascading gauge theory [28, 29], the Sakai-Sugimoto model [30, 31], and various bottom-up models (for example, [32]). Turning on additional deformations which can be studied both in lattice QCD and in strongly coupled holographic models, such as a non-zero isospin chemical potential, could also be instructive. Such work is left for the future.

ACKNOWLEDGMENTS

This work was supported, in part, by the DFG (Emmy Noether Programme EN 1064/2-1) and by the U. S. Department of Energy grants DE-SC-0012447 and DE-SC0011637. LY gratefully acknowledges the hospitality of the University of Regensburg and generous support from the Alexander von Humboldt foundation.

Appendix A: Magnetic field matching at high temperature

To define an optimal matching of the high temperature magnetoresponse in QCD and $\mathcal{N}=4$ SYM, we focus on the entropy density $s = -\partial f/\partial T|_\mu$, as this quantity is independent of the choice of renormalization point μ . As discussed in Ref. [17], at asymptotically high temperature where T is the only relevant physical scale, the renormalization group equation (18) for the QFT free energy density (namely $\mu \frac{d}{d\mu} f = b_1 B^2$) plus dimensional analysis implies that $f = f_0 T^4 - b_1 B^2 [\ln(T/\mu) + \text{const.}] + \mathcal{O}(B^4)$, where $f_0 T^4$ is the free energy density at zero magnetic field. Consequently, the entropy density has the form

$$s = s_0 + b_1 B^2/T + \mathcal{O}(B^4). \quad (\text{A1})$$

For three flavor QCD at temperatures $T \gg \Lambda_H$, asymptotic freedom implies that the entropy density approaches the Stefan-Boltzmann limit, so $s_0 = \frac{19}{9}\pi^2 T^3$. And from Eq. (15a),

the EM β -function coefficient $b_1 = 1/(6\pi^2)$. Hence,⁸

$$\frac{s}{T^3} = \frac{19\pi^2}{9} + \frac{B^2}{6\pi^2 T^4} + \mathcal{O}(B^4). \quad [\text{QCD}] \quad (\text{A2a})$$

For $\mathcal{N}=4$ SYM at strong coupling, the zero field entropy density $s_0 = (N_c^2 - 1) \frac{\pi^2}{2} T^3$ and, with the charge assignments (25), the $U(1)$ β -function coefficient $b_1 = (N_c^2 - 1)/(4\pi^2)$. If these charge assignments are rescaled by an inverse factor of ξ , then

$$\frac{s}{T^3} = (N_c^2 - 1) \left[\frac{\pi^2}{2} + \frac{B^2}{4\pi^2 \xi^2 T^4} + \mathcal{O}(B^4) \right]. \quad [\mathcal{N}=4 \text{ SYM}] \quad (\text{A2b})$$

Matching the relative contribution of the $\mathcal{O}(B^2)$ term in the entropy density, i.e., demanding that $s(B, T)/s(0, T)$ coincide up to $\mathcal{O}(B^4)$, leads to $\xi^2 = 19/3$, or $\xi \approx 2.5$.

[1] E. Witten, *Anti-de Sitter space, thermal phase transition, and confinement in gauge theories*, *Adv. Theor. Math. Phys.* **2** (1998) 505 [[hep-th/9803131](#)].

[2] O. Aharony, S. S. Gubser, J. M. Maldacena, H. Ooguri and Y. Oz, *Large N field theories, string theory and gravity*, *Phys. Rept.* **323** (2000) 183 [[hep-th/9905111](#)].

[3] O. DeWolfe, S. S. Gubser, C. Rosen and D. Teaney, *Heavy ions and string theory*, *Prog. Part. Nucl. Phys.* **75** (2014) 86 [[1304.7794](#)].

[4] A. Adams, L. D. Carr, T. Schaefer, P. Steinberg and J. E. Thomas, *Strongly correlated quantum fluids: ultracold quantum gases, quantum chromodynamic plasmas, and holographic duality*, *New J. Phys.* **14** (2012) 115009 [[1205.5180](#)].

[5] P. M. Chesler and L. G. Yaffe, *Holography and colliding gravitational shock waves in asymptotically AdS_5 spacetime*, *Phys. Rev. Lett.* **106** (2011) 021601 [[1011.3562](#)].

[6] P. M. Chesler and L. G. Yaffe, *Horizon formation and far-from-equilibrium isotropization in supersymmetric Yang-Mills plasma*, *Phys. Rev. Lett.* **102** (2009) 211601 [[0812.2053](#)].

[7] R. A. Janik and R. B. Peschanski, *Asymptotic perfect fluid dynamics as a consequence of AdS/CFT* , *Phys. Rev.* **D73** (2006) 045013 [[hep-th/0512162](#)].

[8] P. M. Chesler and L. G. Yaffe, *Boost invariant flow, black hole formation, and far-from-equilibrium dynamics in $\mathcal{N}=4$ supersymmetric Yang-Mills theory*, *Phys. Rev.* **D82** (2010) 026006 [[0906.4426](#)].

⁸ There is a typo in the expression for s/T^3 in Eq. (4.9) of Ref. [17], which is corrected here.

- [9] P. M. Chesler and L. G. Yaffe, *Holography and off-center collisions of localized shock waves*, *JHEP* **10** (2015) 070 [[1501.04644](#)].
- [10] D. Kharzeev, *Parity violation in hot QCD: Why it can happen, and how to look for it*, *Phys. Lett. B* **633** (2006) 260 [[hep-ph/0406125](#)].
- [11] D. E. Kharzeev, K. Landsteiner, A. Schmitt and H.-U. Yee, ‘Strongly interacting matter in magnetic fields’: an overview, *Lect. Notes Phys.* **871** (2013) 1 [[1211.6245](#)].
- [12] S. Waeber, A. Schäfer, A. Vuorinen and L. G. Yaffe, *Finite coupling corrections to holographic predictions for hot QCD*, *JHEP* **11** (2015) 087 [[1509.02983](#)].
- [13] S. Waeber and A. Schäfer, *Studying a charged quark gluon plasma via holography and higher derivative corrections*, [1804.01912](#).
- [14] M. Panero, *Thermodynamics of the QCD plasma and the large- N limit*, *Phys. Rev. Lett.* **103** (2009) 232001 [[0907.3719](#)].
- [15] G. S. Bali, F. Bursa, L. Castagnini, S. Collins, L. Del Debbio, B. Lucini et al., *Mesons in large- N QCD*, *JHEP* **06** (2013) 071 [[1304.4437](#)].
- [16] G. S. Bali, F. Bruckmann, G. Endrődi, F. Gruber and A. Schäfer, *Magnetic field-induced gluonic (inverse) catalysis and pressure (an)isotropy in QCD*, *JHEP* **04** (2013) 130 [[1303.1328](#)].
- [17] G. S. Bali, F. Bruckmann, G. Endrődi, S. D. Katz and A. Schäfer, *The QCD equation of state in background magnetic fields*, *JHEP* **08** (2014) 177 [[1406.0269](#)].
- [18] Y. Nakayama, *Scale invariance vs conformal invariance*, *Phys. Rept.* **569** (2015) 1 [[1302.0884](#)].
- [19] S. Borsanyi, Z. Fodor, C. Hoelbling, S. D. Katz, S. Krieg and K. K. Szabo, *Full result for the QCD equation of state with 2+1 flavors*, *Phys. Lett. B* **730** (2014) 99 [[1309.5258](#)].
- [20] HOTQCD collaboration, A. Bazavov et al., *Equation of state in (2+1)-flavor QCD*, *Phys. Rev. D* **90** (2014) 094503 [[1407.6387](#)].
- [21] J. F. Fuini and L. G. Yaffe, *Far-from-equilibrium dynamics of a strongly coupled non-Abelian plasma with non-zero charge density or external magnetic field*, *JHEP* **07** (2015) 116 [[1503.07148](#)].
- [22] E. D’Hoker and P. Kraus, *Magnetic brane solutions in AdS* , *JHEP* **0910** (2009) 088 [[0908.3875](#)].
- [23] S. Janiszewski and M. Kaminski, *Quasinormal modes of magnetic and electric black branes*

*versus far from equilibrium anisotropic fluids, Phys. Rev. **D93** (2016) 025006 [1508.06993].*

[24] R. Donagi and E. Witten, *Supersymmetric Yang-Mills theory and integrable systems, Nucl. Phys. **B460** (1996) 299 [hep-th/9510101].*

[25] K. Pilch and N. P. Warner, *$\mathcal{N} = 2$ supersymmetric RG flows and the IIB dilaton, Nucl. Phys. **B594** (2001) 209 [hep-th/0004063].*

[26] A. Buchel and J. T. Liu, *Thermodynamics of the $\mathcal{N} = 2*$ flow, JHEP **11** (2003) 031 [hep-th/0305064].*

[27] C. Hoyos, S. Paik and L. G. Yaffe, *Screening in strongly coupled $\mathcal{N} = 2*$ supersymmetric Yang-Mills plasma, JHEP **10** (2011) 062 [1108.2053].*

[28] I. R. Klebanov and M. J. Strassler, *Supergravity and a confining gauge theory: Duality cascades and χ SB resolution of naked singularities, JHEP **08** (2000) 052 [hep-th/0007191].*

[29] O. Aharony, A. Buchel and P. Kerner, *The black hole in the throat: thermodynamics of strongly coupled cascading gauge theories, Phys. Rev. **D76** (2007) 086005 [0706.1768].*

[30] H. Isono, G. Mandal and T. Morita, *Thermodynamics of QCD from Sakai-Sugimoto model, JHEP **12** (2015) 006 [1507.08949].*

[31] T. Sakai and S. Sugimoto, *Low energy hadron physics in holographic QCD, Prog. Theor. Phys. **113** (2005) 843 [hep-th/0412141].*

[32] M. Attems, J. Casalderrey-Solana, D. Mateos, I. Papadimitriou, D. Santos-Oliván, C. F. Sopuerta et al., *Thermodynamics, transport and relaxation in non-conformal theories, JHEP **10** (2016) 155 [1603.01254].*